

Novel rubidium polyfluorides with F_3, F_4, and F_5 species

Ziyue Lin(林子越), Hongyu Yu(于洪雨), Hao Song(宋昊), Zihan Zhang(张子涵), Tianxiao Liang(梁天笑), Mingyang Du(杜明阳), and Defang Duan(段德芳)

Citation: Chin. Phys. B, 2021, 30 (**6**): 066102. DOI: 10.1088/1674-1056/abefc6
Journal homepage: http://cpb.iphy.ac.cn; http://iopscience.iop.org/cpb

What follows is a list of articles you may be interested in

Ground-state structure and physical properties of YB_3 predicted from first-principles calculations

Bin-Hua Chu(初斌华), Yuan Zhao(赵元), and De-Hua Wang(王德华)
Chin. Phys. B, 2021, 30 (**4**): 046101. DOI: 10.1088/1674-1056/abcf94

Ab initio study on crystal structure and phase stability of ZrC_2 under high pressure

Yong-Liang Guo(郭永亮), Jun-Hong Wei(韦俊红), Xiao Liu(刘潇), Xue-Zhi Ke(柯学志), and Zhao-Yong Jiao(焦照勇)
Chin. Phys. B, 2021, 30 (**1**): 016101. DOI: 10.1088/1674-1056/abb3e7

Synthesis, structure, and properties of $Ba_9Co_3Se_{15}$ with one-dimensional spin chains

Lei Duan(段磊), Xian-Cheng Wang(望贤成), Jun Zhang(张俊), Jian-Fa Zhao(赵建发), Li-Peng Cao(曹立朋), Wen-Min Li(李文敏), Run-Ze Yu(于润泽), Zheng Deng(邓正), Chang-Qing Jin(靳常青)
Chin. Phys. B, 2020, 29 (**3**): 036102. DOI: 10.1088/1674-1056/ab69ea

Isostructural phase transition-induced bulk modulus multiplication in dopant-stabilized ZrO_2 solid solution

Min Wang(王敏), Wen-Shu Shen(沈文舒), Xiao-Dong Li(李晓东), Yan-Chun Li(李延春), Guo-Zhao Zhang(张国召), Cai-Long Liu(刘才龙), Lin Zhao(赵琳), Shu-Peng Lv(吕舒鹏), Chun-Xiao Gao(高春晓), Yong-Hao Han(韩永昊)
Chin. Phys. B, 2019, 28 (**7**): 076109. DOI: 10.1088/1674-1056/28/7/076109

Quantum density functional theory studies of structural, elastic, and opto-electronic properties of $ZMoO_3$ (Z=Ba and Sr) under pressure

Saad Tariq, A A Mubarak, Saher Saad, M Imran Jamil, S M Sohail Gilani
Chin. Phys. B, 2019, 28 (**6**): 066101. DOI: 10.1088/1674-1056/28/6/066101

Novel rubidium polyfluorides with F_3, F_4, and F_5 species*

Ziyue Lin(林子越), Hongyu Yu(于洪雨), Hao Song(宋昊), Zihan Zhang(张子涵), Tianxiao Liang(梁天笑), Mingyang Du(杜明阳), and Defang Duan(段德芳)†

State Key Laboratory of Superhard Materials, College of Physics, Jilin University, Changchun 130012, *China*

(Received 19 February 2021; revised manuscript received 14 March 2021; accepted manuscript online 18 March 2021)

Pressure has an important effect on chemical bonds and their chemical properties. The atypical compounds $NaCl_3$ and CsF_3 are predicted to be stable at high pressure and show unique physical and chemical properties. By using *ab initio* random structure searching and density functional theory calculations, we predicted multiple thermodynamically stable atypical compounds, which are RbF_2, RbF_3, RbF_4, and RbF_5 in the pressure range of 0–300 GPa. In these stable compounds, homonuclear bondings of F_3, F_4, and F_5 species are easily formed. The electron structure calculation showed that except for *Fd*-3*m* phase of RbF_2, these stable compounds are insulators and F 5p orbitals play an important role in the Fermi level. It is interesting that the compounds RbF_5 could be stable at nearly ambient pressure and 0 K which will stimulate experimental studies in the future.

Keywords: high pressure, crystal structure, electron properties, chemical bonds

PACS: 61.50.Ks, 71.20.–b, 82.33.Pt **DOI:** 10.1088/1674-1056/abefc6

1. Introduction

Pressure can greatly shorten interatomic distances, modify chemical properties of elements, overcome reaction barriers, and lead to the formation of some unusual stoichiometric compounds that are difficult to achieve under ambient conditions.[1–3] The new compounds appeared at high pressure usually exhibit novel properties and behaviors.[4–7] For example, mixed H and S can yield an H_3S compound at high pressure with a high critical temperature T_c of 203 K.[8] Similarly, a large variety of atypical compounds, such as $NaCl_3$ with linear $[Cl_3]^-$ species,[9] CsF_3 with high oxidation states have been predicted or synthesized under high pressure.[10]

In recent years, a large variety of atypical polyhalides with unusual bonding and electronic properties, such as $NaCl_3$, KCl_3,[11] KBr_3, KBr_5,[12] CsI_3,[13] etc., have been reported under high pressure. High pressure is a powerful tool to study the structure transformation.[14,15] $NaCl_3$ with linear $[Cl_3]^-$ species has been reported to be stable with *Pnma* phase between 20 GPa and 48 GPa through theoretical prediction and experimental synthesis. At 48 GPa, it transforms from *Pnma* to *Pm*-3*n* phase. In the K–Br system, KBr_3, which formed in a chemical reaction between KBr and Br_2 above 2 GPa at room temperature, has been reported to crystallize in the primitive orthorhombic structure (*Pnma*). On further compression, a monoclinic KBr_5 with $P2_1$ space group has been reported at $\sim$ 6.0 GPa which decomposes to a trigonal (*P*-3*c*1) KBr_3 and Br_2 above 14 GPa and 1500 K. CsI_3 has a three-phase structural sequence at high pressure: orthorhombic (*Pnma*) to trigonal (*P*-3*c*1) to a cubic (*Pm*-3*n*) phase.

On the other hand, a large number of unexpected oxidation states of d-block elements have been identified in fluorides at high pressure, e.g., $Au^{IV}F_4$, Au^{VI},[16] $Hg^{IV}F_4$, $Ir^{VIII}F_8$,[17] because fluorine (F) has a rather large electronegativity and a small atomic size. Of particular interest is the Cs–F system, at low pressure, some F_3, F_4, and F_5 species are formed in compounds CsF_2, CsF_3, and CsF_5. At higher pressure, Cs exhibits a high oxidation state beyond the +1 in CsF_3 and CsF_5, where Cs takes on the role of a 5p element by opening up its inert 5p shell via the aid of strong oxidant F.[10] The alkali-earth element Ba also shows high oxidation states in BaF_3, BaF_4, and BaF_5 at high pressure.[16]

Rb is adjacent to Cs, which may have some similar chemical properties. The only known RbF has a rocksalt-type (*Fm*-3*m*) structure, which becomes a cesium chloride-type (*Pm*-3*m*) structure at about 3 GPa.[10] The chemical reactions of Rb with fluorine under high pressures maybe exhibit even richer chemistry and new phenomena. Here, we explore the high-pressure phase diagram of Rb–F systems for various RbF_n ($n = 1, 2, \ldots 7$) compositions under high pressure via random structural prediction calculations. Our work shows that, in F-rich RbF_n (n = 2, 3, 4, 5) compounds, F_3, F_4, and F_5 species are stabilized at high pressure. We expect high oxidation states of Rb will be seen under extremely high pressure.

2. Computational details

To find stable RbF_n (n = 1–7) compounds in which F has a high stoichiometric number, we conducted an extensive variable-composition structure search with *ab initio* random structure searching (AIRSS) code[18,19] combining with Cambridge serial total energy package (CASTEP) code.[20]

*Project supported by the National Natural Science Foundation of China (Grant No. 11674122).

†Corresponding author. E-mail: duandf@jlu.edu.cn

© 2021 Chinese Physical Society and IOP Publishing Ltd

We performed structure searching and finally predicted about 72000 structures in total from 10 GPa to 300 GPa. Geometry optimization and electronic properties were calculated by Vienna *ab initio* simulation package (VASP) code.[21] The generalized gradient approximation (GGA)[22] within the framework of Perdew–Burke–Ernzerhof (PBE)[23] was used for the exchange–correlation functional, and projector augmented wave (PAW)[24] potentials were used. The cutoff energy was set to 900 eV, and Monkhorst–Pack k meshes were set to $2\pi \times 0.02$ Å^{-1} to ensure that all enthalpy calculations would be converged to better than 1 meV/atom. Bader charges and ELFs were also calculated by VASP. The crystal orbital Hamilton populations (COHP)[25] were calculated with the LOBSTER[26] package. The phonon calculations were performed with PHONOPY[27] code.

3. Results and discussion

Enthalpy difference per atom for RbF_x is obtained by

$$\Delta H_{\text{atom}}(\text{RbF}_x) = \frac{H(\text{RbF}_x) - H(\text{RbF}) - (x-1)H(F)}{x+1}. \quad (1)$$

Based on the above formula, we calculated the enthalpy difference of the most stable phase of RbF_x ($x = 1$–7) relative to RbF and F (*Cmca*) and constructed the convex hull at the pressures of 0, 10 GPa, 50 GPa, 100 GPa, 200 GPa, and 300 GPa presented in Fig. 1(a). In general, structures falling on the convex hull line are thermodynamically stable against decomposition to elemental solids or other binary compounds. To provide more information relevant to experimental synthesis, we built a pressure–composition phase diagram of the Rb–F system, as depicted in Fig 1(b). At ambient pressure, we reproduced the experimentally known RbF structure with the space group *Fm*-3*m*. In additon to RbF, we found that RbF_2, RbF_3, and RbF_5 are thermodynamically stable at ambient pressure. However, RbF_2 and RbF_3 are dynamically unstable due to the imaginary frequencies in their phonon spectra (showed in Fig. S2). As pressure increases, RbF_4 appears on the convex hull in the pressure range between 4 GPa and 75 GPa indicating that it is thermodynamically stable. RbF_2 is stable up to 225 GPa, while RbF_3 and RbF_5 first decompose and then become stable at much high pressure. Both RbF_6 and RbF_7 are unstable within the pressure range studied.

All of the stable compounds undergo a series of phase transitions. The enthalpy difference of stable compounds as a function of pressure is shown in Fig. S1 of the supporting material. Except for *I*4/*mmm* phase of RbF_2 and *Pbam*-0 phase of RbF_3, all of these thermodynamically stable structures have been found to be dynamically stable within their stable pressure ranges, see Fig. S2 in the supporting material.

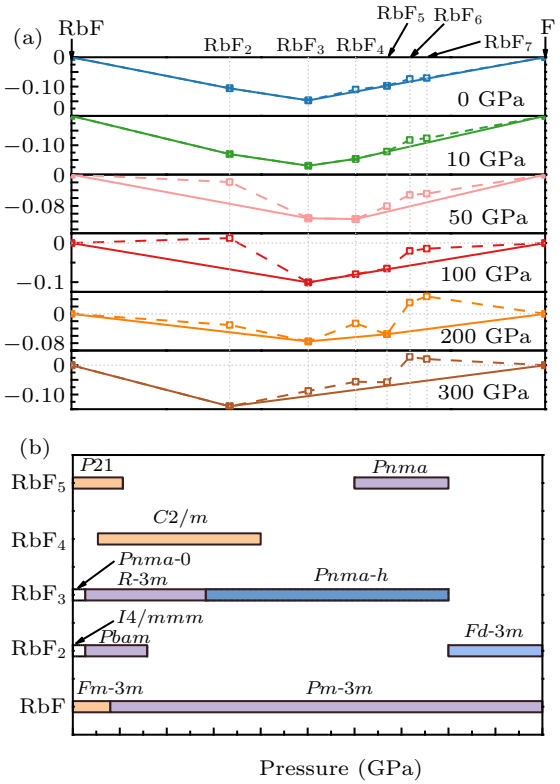


Fig. 1. (a) Convex hull diagram of Rb–F system from 0 to 300 GPa. Dotted lines connect data points, solid lines connect the convex hull. Solid squares represent stable compounds; open squares denote metastable compounds. (b) Pressure–composition phase diagram of Rb–F compounds from 0 to 300 GPa.

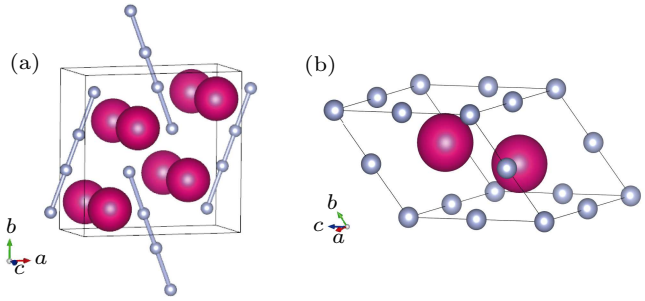


Fig. 2. Crystal structures of RbF_2. (a) *Pbam* RbF_2 structure at 10 GPa, (b) *Fd*-3*m* RbF_2 structure at 250 GPa.

First, let us look at RbF_2, it is stable with tetragonal *Pbam* symmetry at 2 GPa containing F_4 species (Fig. 2(a)). Therefore, the compound can be viewed as $[Rb]_2^+[F_4]^{2-}$ complex. The spacing between F and F atoms in the linear F_4^- species (F_a–F_b–F_c–F_d) is not equal. The distance between the middle two fluorine atoms (F_b–F_c) is 1.68 Å, which has a weaker bonding than that in the pure F_2 molecule (F–F bond length 1.442 Å). For two pairs of fluorine atoms on either side of the F_4 species (F_a–F_b, F_c–F_d), their distances are both 2.02 Å, indicating there is a much weaker bonding than F_b–F_c. Our calculations for Bader charge showed that the charge transfer is 0.63*e* for F_a or F_d, and 0.26*e* for F_b or F_c. This means that the F atom on the side is more likely to ionize. The calculated ICOHP values are −0.676 between F_a and F_b (also F_c and F_d), −2.310 between F_b and F_c. The latter value is much larger

than the former one, indicating that the bonding between the two middle atoms are obviously stronger than the side ones. Interestingly, the configuration of F_4 species in RbF_2 is very similar to that of CsF_2. RbF_2 becomes unstable above 15 GPa, then turns to be stable with a *Fd*-3*m* phase at 225 GPa. This structure is a typical ionic phase (Fig. 2(c)), and the ICOHP of the nearest F–F is −0.267, indicating none existence of F–F covalent bond.

Then we look at RbF_3, it adopts a *R*-3*m* space group at 2 GPa, and transforms to a *Pnma* phase at the pressure of 40 GPa, and keeps stable up to 225 GPa. The *R*-3*m* structure contains linearly symmetric F_3 species with the configuration of $Rb^+[F_3]^-$. Through Bader analysis, Rb^+ transfers 0.93*e* to $[F_3]^-$, and F atoms at both ends of the F_3^- species are equivalent. In such a linear structure, the distance of F–F is 1.71 Å at 10 GPa, with the ICOHP value of −2.02. The F–F bond here is obviously weaker than the F–F bond in the pure F_2 molecule (1.442 Å) , but a little stronger than the F–F bond in *R*-3*m* CsF_3 (1.736 Å).[28]

For the *Pnma* structure, the $[F_3]^-$ species is not linear with the F–F–F angle of 174.267° and its Bader charge is 0.88*e*. We also calculated ICOHPs of the two F–F bonds in F_3 species. Between them, the ICOHP is −2.169 with bond length of 1.68 Å, and the ICOHP is −2.280 with bond length of 1.67 Å.

We found that RbF_4 compound is stable in the pressure range of 4–75 GPa with *C*2/*m* symmetry that contains both $[F_3]^-$ and $[F_2]^-$ species. In such a structure, the nearest distance of F–F is 1.54 Å in a $[F_2]^-$ species, the second and third nearest distance between F atoms is 1.58 Å and 1.76 Å in a $[F_3]^-$ species, and their ICOHP values are −3.838, −3.206, and −1.502, respectively. Shorter bonds have significantly larger ICOHP values, which is consistent with our common knowledge of the relationship between bond length and bond strength. The Bader charges are −0.89*e* for $[Rb]^+$, 1.25*e* for $[F_2]^-$, and 1.14*e* for $[F_3]^-$, suggesting the formation of $[Rb]^+$, $[F_2]^-$, and $[F_3]^-$. Here, the simultaneous presence of $[F_2]^-$ and $[F_3]^-$ species has been predicted for the first time in alkali metal fluorides. This is in line with Miao's work, which shows that there are multiple different clusters of homonuclear bonds in the same compound.[29]

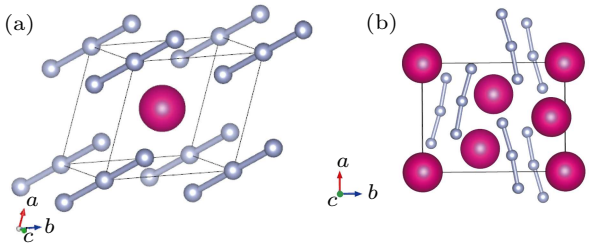


Fig. 3. Crystal structures of RbF_3. (a) *R*-3*m* RbF_2 structure at 10 GPa, (b) *Pnma* RbF_3 structure at 50 GPa.

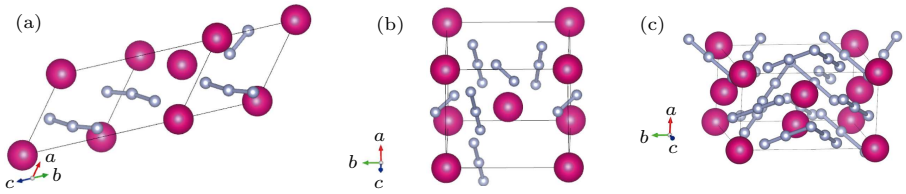


Fig. 4. Crystal structures of RbF_4 and RbF_5. (a) *C*2/*m* RbF_4 structure at 10 GPa, (b) *P*21 RbF_5 structure at ambient pressure, (c) *Pnma* RbF_5 structure at 150 GPa.

In the case of RbF_5, its stable pressure intervals are 0–8 GPa and 150–225 GPa, with the symmetries of $P2_1$ and *Pnma*, respectively. The $P2_1$ structure contains F_3 and F_2 species which have different F–F distances and ICOHPs between atoms: 1.60 Å, ICOHP: −3.182 and 1.82 Å, ICOHP: −1.295 in F_3 species; 1.54 Å, ICOHP: −4.078 in F_2 species. The F_3 group accepts 0.67*e*, F_2 group accepts 0.25*e*, and the Rb atom loses 0.92*e*. The *Pnma* structure has a symmetrical V-shaped $[F_5]^-$ species. This configuration also appears in the CsF_5 with a $P2_1$ symmetry.[28] The Rb transfers 0.86*e* to the F_5 species, suggesting the existence of Rb^+ cation and $[F_5]^-$ anion. We use F_a–F_b–F_c–F_d–F_e to represent a F_5 unit. The distance and ICOHP value between F atoms at 0 GPa are, F_a–F_b: 1.49 Å, ICOHP: −4.363; F_b–F_c: 1.79 Å, ICOHP: −1.041; F_c–F_d: 1.79 Å, ICOHP: −1.041; F_d–F_e: 1.49 Å, ICOHP: −4.363. The F_5 species here is symmetric, and the whole compound can be viewed as $Rb^+[F_5]^-$.

From partial density of states (PDOS), we can tell whether a compound is a conductor, a semiconductor, or an insulator, and can also make a preliminary estimate of the likelihood of bonding between different atoms by the degree of orbital overlap. We calculated PDOS for multiple crystal structures containing F_2, F_3, and F_5 species (Fig. 5). First of all, according to the PDOS values at Fermi level, except for *Fd*-3*m* RbF_2, these predicted stable compounds are insulators (Fig. S3). On the other hand, there is a little overlap between Rb 5p and F 2p states around the Fermi level (Fig. 3(a)), indicating that 5p electrons of Rb are not involved in bonding. From the analysis of Bader charges and PDOS, we can see that there is no potential for finding new oxidation states in our predicted stable Rb–F compounds up to 300 GPa, and a high oxidation state will appear at much higher pressure.

The electron localization function (ELF) is used to characterize the localized distribution of electrons, determine the

type of bonding, and find out the lone pair electron distribution. The ELFs of the stable phases were calculated. Red areas (ELF$\approx$ 1.0) around Rb and F atoms indicate the lone electron pairs, and green areas (ELF$\approx$ 0.5) between the F atoms indicate strong covalent bonding. Blue areas in ELFs typically indicate non-covalent bonding, for example, delocalized electrons in metals. Through this judgment, we further confirm the F_3, F_4, and F_5 species in these structures. We calculated the ELF of all the stable compounds shown in Fig. 6 and Fig. S4. First let us look at the ELF of *Pbam* RbF_2 at ambient pressure, the F_4 cluster exists in a linear form which was also found in the structure of *Pbam* CsF_2.[28] For *R*-3*m* RbF_3, there are linear equivalent F_3 units (Fig. 6(b)). This form of the F_3 unit has been found in other fluorides such as CsF_3.[28] In $C2/m$ RbF_4, the ELF and structure diagram show asymmetric F_2 and F_3 units (Fig. 6(d)). In *Pnma* RbF_5 (Fig. 6(e)), it tends to form symmetrical V-shaped F_5 units, which was also predicted in the work of CsF_5.[28]

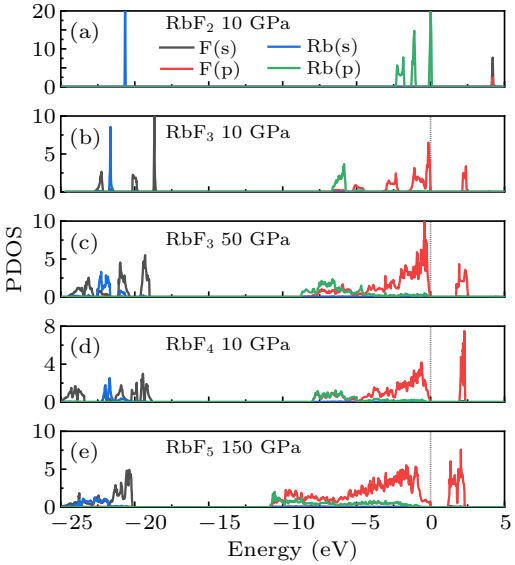


Fig. 5. The calculated PDOS of (a) *Pbam* RbF_2 at 10 GPa, (b) *R*-3*m* RbF_3 at 10 GPa, (c) *Pnma-h* RbF_3 at 50 GPa, (d) *C*2/*m* RbF_4 at 10 GPa, (e) *Pnma* RbF_5 at 150 GPa. The states are aligned at the Fermi level (vertical dashed lines).

In this work, homonuclear covalent bonds like F_3, F_4, and F_5 species form in the Rb–F system, which has been explained by Miao *et al.* using the Hückel model.[29] The atomic orbital energies of the different elements in the heterogenous bond are different, whereas in the homonuclear bond, the two atomic orbitals forming the chemical bond have the same energy, so the bond energy of heterogenous bond formed will be greater than the energy in the homonuclear bond. For the system we study, the case happens to be that F–F bonds are generated preferentially under pressure.

Under the action of pressure, the energy of the inner electron orbital will also increase, and eventually, the inner electrons may achieve enough energy to participate in bonding. Also, the effect of pressure will reduce the energy of electron orbitals that are not occupied, and make such orbitals likely to be involved in bonding.[29] In the case of cesium fluoride, inner-shell electrons become the main components of chemical bonds in a lower pressure range.[10] In the investigation below 300 GPa, we just only found F_3, F_4, and F_5 species in the Rb–F system. If the pressure increases further, high oxidation state of rubidium beyond the +1 state would appear in the novel rubidium fluorides, which will be discussed in the future.

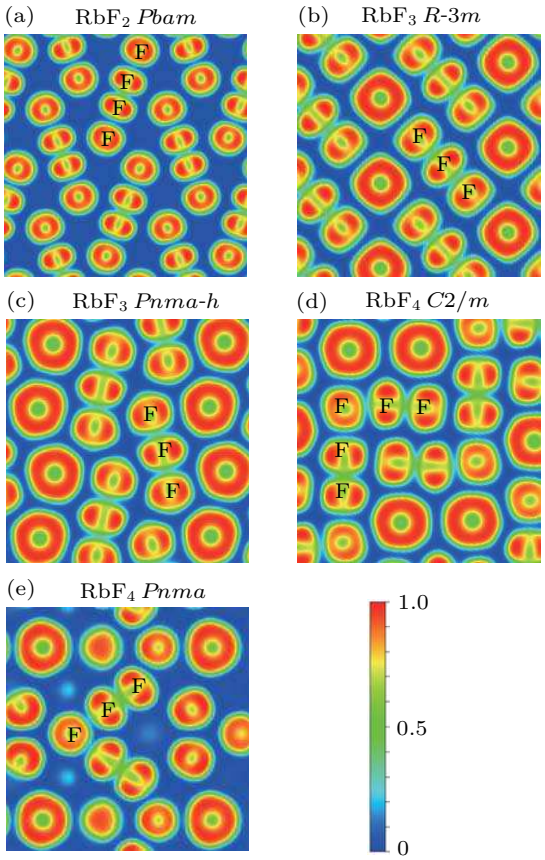


Fig. 6. The ELFs of (a) *Pbam* RbF_2 at 10 GPa, (b) *R*-3*m* RbF_3 at 10 GPa, (c) *Pnma* RbF_3 at 50 GPa, (d) *C*2/*m* RbF_4 at 10 GPa, (e) *Pnma* RbF_5 at 150 GPa.

4. Conclusion

In summary, four new compounds of RbF_2, RbF_3, RbF_4, and RbF_5 were predicted to be stable at experimentally accessible pressures. Based on the bond lengths, Bader charges, ICOHP values, ELFs, and PDOS, we found that the stable rubidium fluorides behave as ionic compounds containing $[F_3]^-$, $[F_4]^{2-}$, and $[F_5]^-$ species under high pressure, and Rb has not been oxidized beyond +1 states up to 300 GPa. The homonuclear bonding of F–F is easily formed at low pressure. After further pressurization, it is prospect for the possibility of the future discovery of Rb with high oxidation states in which inner orbital electrons participate in bonding.

Acknowledgements

Parts of the calculations were performed in the High Performance Computing Center (HPCC) of Jilin University and TianHe-1(A) at the National Supercomputer Center in Tianjin.

References

[1] Sun G L, Huang H M and Li Y L 2016 *Chin. Phys. Lett.* **33** 026104
[2] Zhang J, Liu F L, Dong J K, Xu Y, Li N N, Yang W G and Li S Y 2015 *Chin. Phys. Lett.* **32** 097102
[3] Hai Z, Zhao L X, Hou X Y, Shan L, Ren Z, Chen G F and Ren C 2020 *Chin. Phys. Lett.* **37** 097403
[4] Zhang Y L, Hao X Z, Huang Y P, Tian F B, Li D, Wang Y C, Song H and Duan D F 2021 *Chin. Phys. Lett.* **38** 026101
[5] Xu J M, Wang S Y, Wang W J, Zhou Y H, Chen X L, Yang Z R and Qu Z 2020 *Chin. Phys. Lett.* **37** 076202
[6] Wang C, Liu Y X, Chen X, Lv P and Liu X B 2020 *Chin. Phys. Lett.* **37** 026201
[7] Tian C, Huang X L, Huang Y P, Li X, Zhou D, Wang X and Cui T 2019 *Chin. Phys. Lett.* **36** 106101
[8] Duan D, Liu Y, Tian F, Li D, Huang X, Zhao Z, Yu H, Liu B, Tian W and Cui T 2014 *Sci. Rep.* **4** 6968
[9] Zhang W, Oganov A R, Goncharov A F, zhu Q, Boulfelfel S E, Lyakhov A O, Stavrou E, Somayazulu M, Prakapenka V B and Konopkova Z 2013 *Science* **342** 1502
[10] Miao M S 2013 *Nat. Chem.* **5** 846
[11] Zhang W, Oganov A R, Zhu Q, Lobanov S S, Stavrou E and Goncharov A F 2016 *Sci. Rep.* **6** 26265
[12] Patel N N, Verma A K, Mishra A K, Sunder M and Sharma S M 2017 *Phys. Chem. Chem. Phys.* **19** 7996
[13] Wei S, Wang J, Deng S, Zhang S and Li Q 2014 *Sci. Rep.* **5** 14393
[14] Zhu L Y, Wang P, Zhai C G, Hu K, Yao M G and Liu B B 2019 *Acta. Phys. Sin.* **68** 176101 (in Chinese)
[15] Yuan P F, Zhu W J, Xu J A, Liu S J and Jing F Q 2010 *Acta. Phys. Sin.* **59** 8755 (in Chinese)
[16] Lin J Y, Zhang S T, Guan W, Yang G C and Ma Y M 2018 *J. Am. Chem. Soc.* **140** 9545
[17] Lin J Y, Zhao Z Y, Liu C Y, Zhang J, Du X, Yang G C and Ma Y M 2019 *J. Am. Chem. Soc.* **141** 5409
[18] Pickard C J and Needs R J 2006 *Phys. Rev. Lett.* **97** 045504
[19] Pickard C J and Needs R 2011 *J. Phys.: Condens. Matter* **23** 053201
[20] Segall M D, Lindan P J D, Probert M J, Pickard C J, Hasnip P J, Clark S J and Payne M C 2002 *J. Phys.: Condens. Matter* **14** 2717
[21] Kresse G and Furthmüller J 1996 *Phys. Rev. B* **54** 11169
[22] Perdew J P and Wang Y 1992 *Phys. Rev. B* **46** 12947
[23] Perdew J P, Burke K and Ernzerhof M 1996 *Phys. Rev. Lett.* **77** 3865
[24] Blöchl P E 1994 *Phys. Rev. B* **50** 17953
[25] Dronskowski R and Blöchl P E 1993 *J. Phys. Chem.* **97** 8617
[26] Deringer V L, Tchougréeff A L and Dronskowski R 2011 *J. Phys. Chem. A* **115** 5461
[27] Togo A, Oba F and Tanaka I 2008 *Phys. Rev. B* **78** 134106
[28] Zhu Q, Oganov A R and Zeng Q 2015 *Sci. Rep.* **5** 7875
[29] Miao M S, Sun Y H, Zurek E and Lin H Q 2020 *Nat. Rev. Chem.* **4** 508